Wiley
BioMed Research International
Volume 2025, Article ID 5556353, 16 pages
https://doi.org/10.1155/bmri/5556353

Research Article

Expression of UCOE and HSP27 Molecular Elements to Improve the Stable Protein Production on HEK293 Cells

Concepción Sosa-García, Uriel Abdallah Sánchez-Pacheco, Carlos Alberto Tavira-Montalvan, and Angélica Meneses-Acosta

Laboratory of Pharmaceutical Biotechnology, Faculty of Pharmacy, Autonomous University of the State of Morelos, Cuernavaca, Morelos, Mexico

Correspondence should be addressed to Angélica Meneses-Acosta; angelica_meneses@uaem.mx

Received 20 August 2024; Accepted 11 January 2025

Academic Editor: Rossana C Zepeda

Copyright © 2025 Concepción Sosa-García et al. BioMed Research International published by John Wiley & Sons Ltd. This is an open access article under the terms of the Creative Commons Attribution License, which permits use, distribution and reproduction in any medium, provided the original work is properly cited.

Recombinant proteins represent one of the greatest achievements of modern pharmaceutical biotechnology, as they are increasingly used across nearly all branches of medicine to treat a wide range of conditions. In response to this demand, various cell engineering approaches have been developed to improve their expression. Some of these approaches involve the use of genetic elements that prevent the silencing of the gene of interest, as well as the generation of resistant cell lines to inhibit or avoid programmed cell death (PCD). This research focuses on analyzing the effects of overexpression of UCOE elements and the HSP27 protein, both individually and together, on the production of human rIFNγ in HEK293 cells. Our results show that 4-Kb UCOE elements have no effect on protein production in HEK293 cells, while overexpression of HSP27 prolongs the stationary phase during growth kinetics. The Qp of rIFNγ is 96-fold higher in clones containing the HSP27/UCOE combination compared to the clone containing only UCOE elements or to the control HEK293 cells. These results correlate with the MCP analyses, which showed that overexpression of HSP27 decreased the expression of Bax, caspase 3, cytochrome C, Beclin, and LC3II mRNA. Finally, this study suggests the potential utility of a cell engineering approach based on the overexpression of the human HSP27 protein for enhancing the production of recombinant viruses and proteins in HEK293 cells.

Keywords: apoptosis; autophagy; HEK293; HSP27; IFNγ; programmed cell death; UCOE

1. Introduction

The significant achievement of recombinant therapeutic proteins (RTPs) in modern medicine underscores the need for continuous improvement in their production processes to meet growing therapeutic demands. The demand for RTPs has surged, with the FDA and EU approving 178 products from 2015 to 2019 and 117 products from January 2020 to June 2022 [1]. This growth is largely attributed to mammalian cell–based production platforms, which provide essential posttranslational modifications, such as glycosylation, that influence the quality, efficacy, and safety of these biopharmaceuticals [2]. To address this increasing demand, innovative strategies are being explored to enhance expression levels in animal cell cultures, previously seen as limited for production. Key goals include boosting cell viability, viable cell density, and cell-specific production rates to ensure a reliable supply of high-quality RTPs [3].

Epigenetic silencing of genes significantly contributes to the loss of productivity in recombinant protein production. This silencing occurs through modifications such as hypermethylation of CpG sequences and histone hypoacetylation [4, 5]. To address this, molecular strategies involving elements that counteract these effects are essential. Novel expression vectors incorporating genetic elements, such as insulators, have been developed to prevent the spread of repressive chromatin [6], including UCOE vectors. UCOE elements are nucleotide sequences that provide stable, integration-independent transgene expression, even in heterochromatin regions like centromeres [7]. These elements

consist of two promoters from the housekeeping genes HNRPA2B1 and CBX3, surrounded by methylation-free CpG islands and euchromatic histone marks, which promote stable gene expression.

The incorporation of UCOE elements into expression vectors has been shown to significantly improve recombinant protein production in some cases [8–10]. While such approaches have primarily been explored in animal cell systems such as CHO cells, there is increasing interest in applying them to other platforms, such as HEK293 cells. This may offer significant advantages to the biotechnology industry, highlighting the potential of UCOE elements to improve transgene expression in various production systems.

On the other hand, molecular strategies targeting the modulation of genes related to programmed cell death (PCD) are employed to enhance cell development and improve bioprocess outcomes [11]. PCD significantly impacts bioprocesses by reducing cell viability and product quality. To address this, genes involved in PCD regulation are either inserted or deleted to extend the lifespan of cell cultures. This includes downregulating or deleting proapoptotic genes such as Bax, Bak, caspase 3, and caspase 7 [12–14] and overexpressing antiapoptotic genes from the B cell lymphoma protein family, such as Bcl-xL and Bcl-2 [15–17]. Additionally, heat shock proteins such as HSP27 are utilized in these strategies to further support cell survival and productivity. HSP27 is a crucial chaperone involved in cytoskeletal stability, protein synthesis, redox potential, and apoptosis modulation [18]. Recent studies suggest its involvement in autophagy, although it is primarily studied as a biomarker for cancer and neurodegenerative diseases [19, 20]. Molecular applications have shown that overexpression of HSP27 in murine systems modulates apoptosis pathways and delays caspase activity, enhancing the specific productivity of target proteins [21, 22].

Finally, HEK293 cells are used industrially for producing recombinant proteins, virus-like particles (VLPs), and viral vectors for biopharmaceuticals, vaccines, and gene therapy products [23, 24]. This cell line was originally derived from human embryonic kidney cells and subsequently transfected with the E1 region of Adenovirus Type 5, which was integrated into Chromosome 19 [25, 26]. HEK293 cells, being of human origin, can perform posttranslational modifications, such as glycosylation, that are similar to those in humans [27], which is a major advantage. Additionally, these cells can be adapted to grow in both suspension and adherent cultures [28]. However, some challenges remain, such as their productivity compared to CHO cells.

Based on the above, this study focuses on analyzing the effect of UCOE elements and HSP27 protein expression, both individually and together, as potential molecular tools for the development of stable HEK293 cell clones, with a direct impact on recombinant proteins production.

2. Materials and Methods

To improve the productivity of biopharmaceuticals using HEK2923 cells, various molecular strategies have been employed. In this context, UCOE elements and the HSP27 protein have shown promise as molecular targets for enhancing productivity in CHO cells. However, there is limited scientific evidence analyzing the productivity of these elements individually, and no evidence exists regarding their combined effect within the HEK293 production system. This underscores the importance of conducting such an analysis, as presented in our study. For this purpose, different stable expression clones were generated: HEK293/UCOE (HEK/UCOE) clone and HEK293/HSP27 (HEK/27) clone for the analysis of each strategy separately and the HEK293/HSP27/UCOE (HEK/27/U) clone for the synergistic evaluation. To obtain these clones, two expression vectors were constructed.

2.1. Genetic Vector Construction. Two expression vectors were created: the UCOE/rIFNγ vector using the UCOE-Human 4Kb Puro Set expression vector from Merck and the TOPO/HSP27 vector using the pcDNA3.3-TOPO plasmid. The human HSP27 gene (GenBank Accession No. NM_001540.5) was obtained from the Frt-hspB1 vector. For the human IFNγ gene (GenBank Accession No. NM_000619.3), the pVAX1/IFNγ vector was used, along with the oligos listed in Table 1. The human IFNγ gene encodes for the model transgenic IFNγ protein, a dimerized soluble cytokine weighing between 15.5 and 25 kDa. The protein possesses native N-glycosylation at residues N25 and N97, as well as an N-terminal pyroglutamate residue.

2.1.1. Vector Construction and Characterization. The transgene inclusions (IFNγ and HSP27) required to generate the respective vectors were performed using PCR reactions with the oligos listed in Table 1. The integrity of the gene sequences was confirmed at the DNA Synthesis and Sequencing Unit (USSDNA) of the IBT-UNAM. The obtained sequences were analyzed by Chromas 2.6.6 (https://technelysium.com.au/wp/chromas/) and Blast from NCBI (https://blast.ncbi.nlm.nih.gov/blast/Blast.cgi).

2.2. Cell Cultures. Adherent cultures of human embryonic kidney cells (HEK293, ATCC CRL-1573) were maintained in D-MEM/F-12 medium (Gibco) supplemented with 10% (vol/vol) fetal bovine serum (FBS). The cultures were incubated at 37°C and 5% CO_2. Cell Passage Number 8 was used for the experiments to ensure a low passage number and minimize the risk of genetic modifications.

2.2.1. Clone Generation for Stable Expression. Three stable clones were constructed: HEK293/UCOE, HEK293/HSP27, and HEK293/HSP27/UCOE. The HEK293/UCOE and HEK293/HSP27 clones were generated via lipofection using Lipofectamine 2000 (Lipofectamine 2000, Thermo Fisher Scientific) following the manufacturer's instructions. The HEK293/HSP27 clone was subsequently retransfected with the UCOE/rIFNγ vector to generate the HEK293/HSP27/UCOE clone. Prior to transfection, the vectors were linearized using specific restriction enzymes. Monoclonal selection was performed using the limiting dilution technique. The selection medium consisted of DMEM/F12 (10% SFB) with Puromycin (Sigma, Ref. P9620) was used for selecting UCOE/rIFNγ clones, while Geneticin (Gibco, Ref. 10131–

Table 1: Designed oligos for RT-PCR reactions.

Gene	Amplicon (bp)	Sequence	Reference
Oligos used for vector construction and clonal evaluation			
Human IFNγ	516	Fwd: 5′-CGGCGGCCGGCCGATGAAATATACAAGTTATATC-3′ Rev: 5′-CTTGTTAGCTAGCTTACTGGGATGCTCTTCGAC-3′	NA
Human HSP27	662	Fwd: 5′-CTTTAATAGGCCGGCCTCGAGAGCATGACCGAGCG-3′ Rev: 5′-CTTAATTAGGCCGGCCGCGTTTACTTGGCGGCAG-3′	NA
RT-PCR HSP27	142	Fwd: 5′-GTCCCTGGATGTCAACCACTTC-3′ Rev: 5′-CAGCGRGTATTTCCGCGTGAAG-3′	NA
Apoptosis genes			
Cleaved caspase 3	170	Fwd: 5′-AAGCGAATCAATGGACTCTGG-3′ Rev: 5′-GAATGTTTCCCTGAGGTTTGC-3′	[29]
Bax	195	Fwd: 5′-TGGCAGCTGACATGTTTTCTGAC-3′ Rev: 5′-TCACCCAACCACCCTGGTCTT-3′	[30]
Cytochrome C	132	Fwd: 5′-GGGCGAGAGCTATGTAATGCAAG-3′ Rev: 5′-TACAGCCAAAGCAGCAGCTCA-3′	[31]
Autophagy genes			
Beclin 1	191	Fwd: 5′-CAAGATCCTGGACCGTGTCA-3′ Rev: 5′-TGGCACTTTCTGTGGACATCA-3′	[32]
LC3II	167	Fwd: 5′-GATGTCCGACTTATTCGAGAGC-3′ Rev: 5′-TTGAGCTGTAAGCGCCTTCTA-3′	[33]
p53 and constitutive genes			
p53	90	Fwd: 5′-TGCGTGTGGAGTATTTGGATG-3′ Rev: 5′-TGGTACAGTCAGAGCCAACCTC-3′	[34]
GAPDH	161	Fwd: 5′-TTGGCTACAGCAACAGGGTG-3′ Rev: 5′-GGGGAGATTCAGTGTGGTGG-3′	[35]

027) was used for selecting TOPO/HSP27 clones. A stable clone was defined as one maintaining viability for more than 16 generations under selective pressure.

2.2.2. Clonal Evaluation. To confirm the successful generation of each clone, the presence of rIFNγ and HSP27 messenger RNA was verified using RT-PCR for the corresponding clones. Total RNA was extracted using TRIZOL (TRI Reagent, Zymo Research Cat. No. R2050-1–50) following the manufacturer's instructions. Genomic DNA was removed using the DNaseI enzyme (Thermo Scientific, Cat. No. EN0521). Complementary DNA (cDNA) synthesis was performed with RevertAid H Minus First Strand cDNA Synthesis kit (Thermo Scientific, Cat. No. K1631). The oligonucleotides used to amplify IFNγ and HSP27 cDNA are listed in Table 1.

rIFNγ by the HEK293/UCOE and HEK293/HSP27/UCOE selected clones was quantified using ELISA with the Human IFN gamma ELISA Kit (Invitrogen, BMS228), following the manufacturer's instructions.

2.2.3. Effect of UCOE and HSP27 Elements on the Production of Recombinant Proteins. To evaluate the effect of the individual or combined expression of UCOE and HSP27 elements on the production of rIFNγ, the growth kinetics of each obtained clone were analyzed. Cell viability and kinetic and metabolic parameters were determined for each clone. rIFNγ was quantified using the ELISA method to calculate volumetric production and specific productivity (Qp). A detailed description is provided below.

2.2.3.1. Kinetic and Metabolic Profiling of HEK293/UCOE, HEK293/HSP27, and HEK293/HSP27/UCOE Clones. Production kinetics were evaluated in 12-well plates, where 5×10^4 cells/mL of each generated clone were seeded and cultured in static conditions using DMEM/F-12 medium supplemented with 10% of FBS. The cultures were incubated at 37°C and 5% CO_2 for 12–16 days. Cell pellets were collected every 24 h for cell counting using the trypan blue exclusion method. Culture supernatants were analyzed to quantify the production of human rIFNγ using the Invitrogen Human IFN gamma ELISA Kit (BMS228), following the manufacturer's instructions. Additionally, cell metabolism was assessed by measuring monitored by quantification of glucose, glutamine, lactate, and glutamate levels using the YSI model 2900 analyzer. From the collected data, the volumetric production, Qp, and the kinetic and metabolic parameters of each clone were determined. The results are expressed in relative units, with the HEK293/UCOE clone used as a control, to compare the production levels of human rIFNγ the different clones.

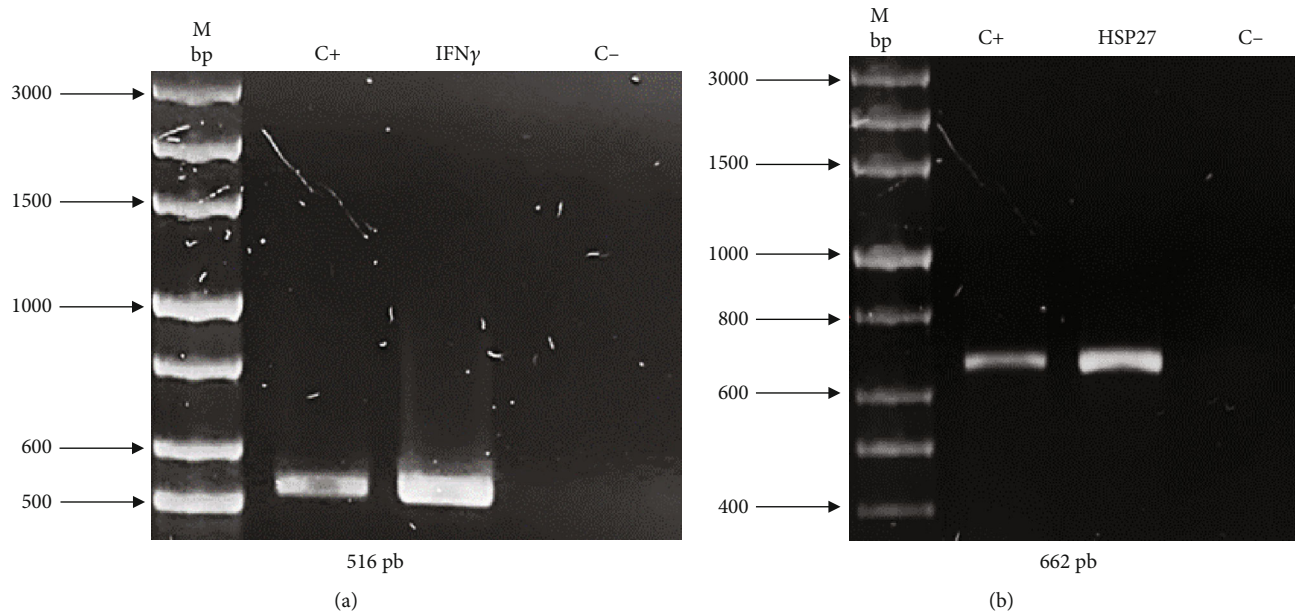

Figure 1: TOPO/HSP27 and UCOE/IFNγ vector constructs. In order to confirm the presence of the HSP27 and human IFNγ genes in the corresponding construct, PCR and sequencing of each vector were performed. (a) PCR of UCOE/IFNγ vector, C+: pVAX1/IFNγ vector, IFNγ: UCOE/IFNγ vector (516 bp). (b) PCR of the TOPO/HSP27 vector, C+: Frt-HSPB1 vector, HSP27: TOPO/HSP27 vector (662 bp). M bp: base pair marker, C–: negative control of the reaction.

Qp was calculated as a function of growth rate (μ) and volumetric productivity using the following equation:

$$\text{Qp} = \mu * \frac{P2 - P1}{N2 - N1}$$

where P represents the volumetric productivity and N is the viable cell density.

2.2.3.2. Evaluation of the Effect of HSP27 as a Modulator of PCD. To assess the impact of HSP27 on PCD, changes in the expression of apoptosis and autophagy-related genes were analyzed using RT-PCR. Additionally, apoptosis and autophagy fluxes were evaluated using dyes such as acridine orange (AO), propidium iodide (PI), and a green fluorescent detection reagent, observed via epifluorescence microscopy. RT-PCR: RNA extraction and conversion to cDNA were performed using standard methods. Specific primers for apoptosis and autophagy-related genes are listed in Table 1.

AO and PI (AO/PI) staining: HEK293 and HEK293/HSP27 cells were cultured on round coverslips in 24-well plates and treated with 0.195 nM staurosporine (STS) to induce apoptosis. The cells were stained with a 1:1 mixture of AO and PI and observed under a Nikon eclipse E400 epifluorescence microscope using TRITC (red) and FITC (green) filters.

Autophagosome staining: HEK293 and HEK293/HSP27 cells were cultured to 90% confluence, washed with PBS, and incubated with fresh medium with or without serum for 48 h. Cells were then treated with the Autophagy Detection Kit (Abcam, ab139484) and observed under a Nikon eclipse E400 epifluorescence microscope, following the manufacturer's protocol.

2.3. Statistics. Results from densitometry and growth kinetics analyses were expressed as the mean ± standard deviation of six samples. Yields were expressed as the mean ± standard error of two samples, while, for volumetric production, a two-way ANOVA ($p < 0.05$) was performed, followed by Tukey's post hoc test. For specific productivity, a one-way ANOVA ($p < 0.05$) was conducted, also followed by Tukey's post hoc test. In both cases, results were expressed as the mean ± standard error of two samples. RT-PCR results were presented as the mean ± standard deviation, and statistical significance was determined using the Mann–Whitney test ($p < 0.05$). Graphs and statistical analysis were performed in GraphPad Prism 9.0 with a significance value < 0.05.

3. Results and Discussion

3.1. Construction and Characterization of UCOE/IFNγ and TOPO/HSP27 Vectors. As previously described, two expression vectors were constructed to demonstrate the effectivity of UCOE and HSP27 protein. The presence of genes of interest (human rIFNγ and HSP27) within the constructs was validated by PCR. Figure 1(a) shows an amplicon of 516 bp corresponding to IFNγ, and Figure 1(b) shows an amplicon of 662 bp corresponding to HSP27. The sequence integrity of the IFNγ and HSP27 genes within the vectors was confirmed by sequencing (Supporting Information). Figure S1 shows the sequencing results for the UCOE/IFNγ plasmid, showing 100% identity of the IFNγ sequence in the UCOE vector with the coding region registered in the NCBI database. Similarly, Figure S2 displays the sequencing results for the TOPO/HSP27 vector, also showing 100% identity of the HSP27 sequence in the TOPO vector with the NCBI database. In both cases, the gene sequence was confirmed to be in the correct reading frame.

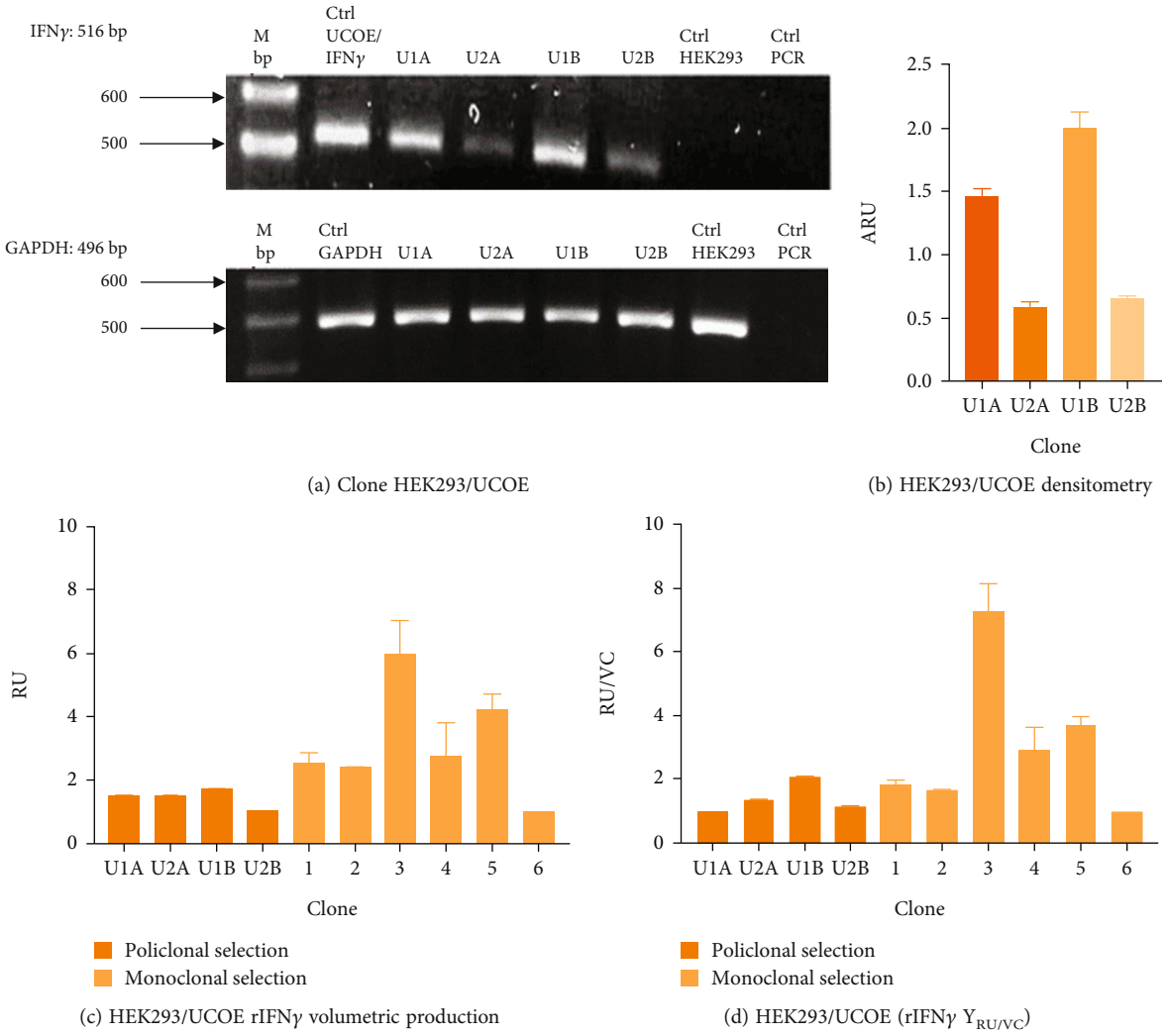

(a) Clone HEK293/UCOE

(b) HEK293/UCOE densitometry

(c) HEK293/UCOE rIFNγ volumetric production

(d) HEK293/UCOE (rIFNγ $Y_{RU/VC}$)

Figure 2: HEK293/UCOE clone evaluation. (a) rIFNγ RT-PCR. U1A: Clone 1A, U2A: Clone 2A, U1B: Clone 1B, U2B: Clone 2B, Ctrl UCOE/rIFNγ: UCOE/rIFNγ construct. (b) Densitometric analysis of HEK293/UCOE clone. Increased expression of human rIFNγ messengers was observed in the U1B clone. Results are expressed as mean ± standard deviation of three samples. (c) Volumetric production of human rIFNγ during polyclonal and monoclonal selection. Results are expressed as the mean ± standard error of two samples. (d) Human rIFNγ yields during polyclonal and monoclonal selection. Results are expressed as mean ± standard error of two samples. During polyclonal selection, a higher production of human rIFNγ was observed in Clone U1B, which was used for monoclonal selection, where Clone 3 was identified as the one with the highest production and was used for subsequent analysis.

Once the presence and integrity of the genes were confirmed, these vectors were used to stably transform HEK293 cells.

3.2. Clonal Evaluation and Selection

3.2.1. HEK293/UCOE. Figure 2(a) shows the RT-PCR results of the polyclonal pools, with an amplicon of 516 bp, confirming the presence of the transgene in the four generated pools (U1A, U2A, U1B, U2B). In this case, the presence of the rIFNγ gene is not observed in the parental cell line, as it is not produced endogenously, and the parental cells were used as a negative control. The mRNA expression level of rIFNγ (Figure 2(b)) was the highest in pool U1B (1.99 ± 0.14 ARU). Additionally, Figures 2(c) and 2(d) show that this pool exhibited high volumetric production and yields of rIFNγ (1.73 ± 0.03 RU and 2.05 ± 0.02 RU/VC, respectively). Based on these results, monoclonal selection was performed from this pool.

To analyze the effect of UCOE elements, the six highest yielding clones derived from monoclonal selection were examined. Figures 2(c) and 2(d) show that the clone with the highest titer and yields was Clone 3 (5.96 ± 0.75 RU and 7.24 ± 0.91 RU/VC, respectively), which exhibited a sevenfold higher yield compared to the lowest-producing clone.

3.2.2. HEK293/HSP7/UCOE. To evaluate the effect of the HSP27 protein in combination with the UCOE elements, four polyclonal pools (1A, 2A, 1B, and 2B) were generated. Figure 3(a) confirms the presence of the HSP27 gene, with an amplicon of 142 bp in all cases. According to the densitometric analysis (Figure 3(b)), Pool 1A shows overexpression of this protein compared to the parental line, likely due to

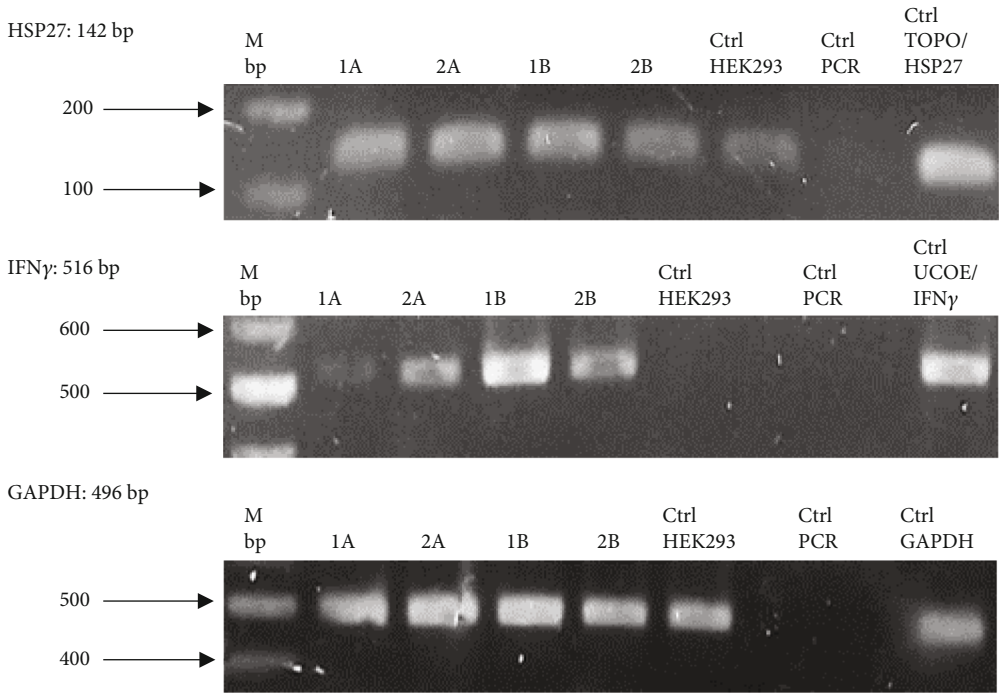

(a) Clone HEK293/HSP27/UCOE

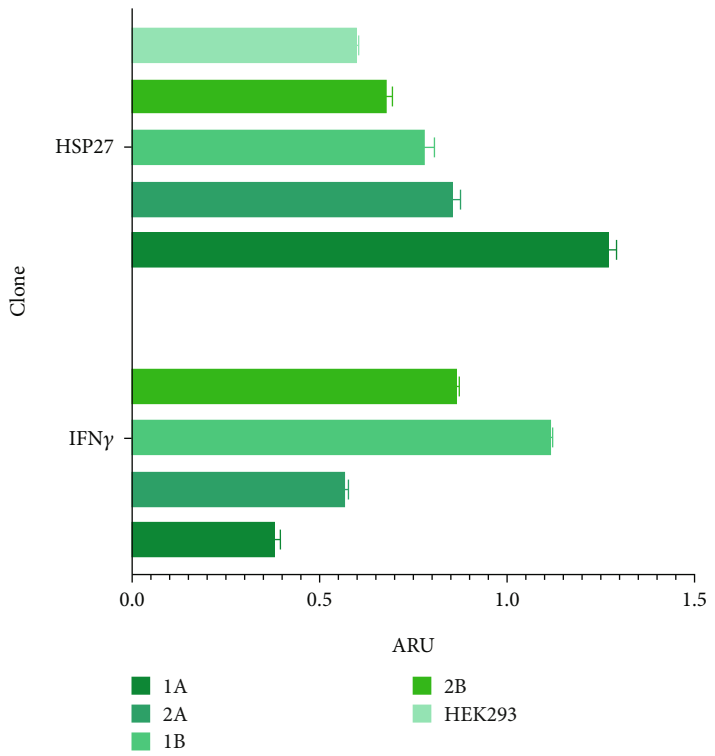

(b) HEK293/HSP27/UCOE densitometry

Figure 3: Continued.

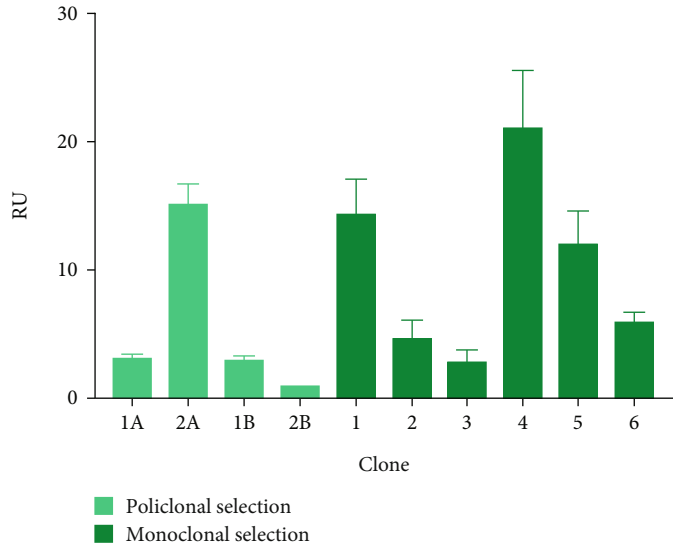

(c) HEK293/HSP27/UCOE rIFNγ volumetric production

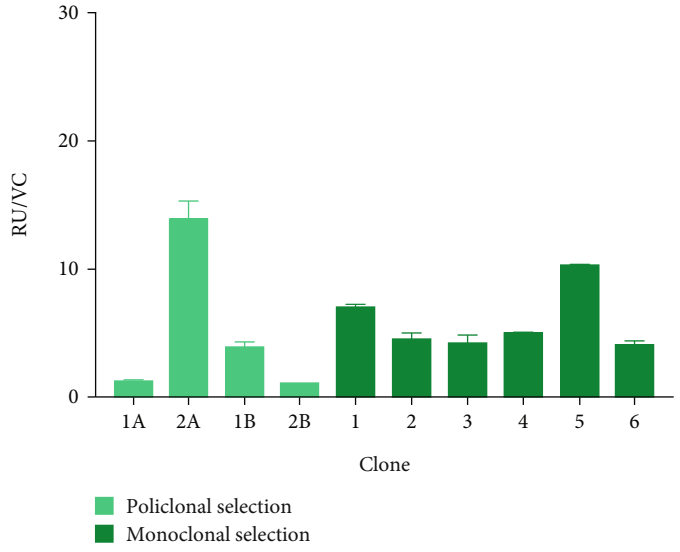

(d) HEK293/HSP27/UCOE (rIFNγ $Y_{RU/VC}$)

Figure 3: HEK293/27/UCOE clone evaluation. (a) rIFNγ and HSP27 RT-PCR. 1A: Clone 1A, 2A: Clone 2A, 1B: Clone 1B, 2B: Clone 2B, Ctrl UCOE/IFNγ: UCOE/IFNγ construct, Ctrl PCR: control of PCR reaction, HSP27 RT-PCR. CA: Clone A, CB: Clone B, Ctrl TOPO/HSP27: TOPO/HSP27 construct, Ctrl HEK293: nontransfected HEK293, Ctrl GAPDH: GAPDH constitutive gene. (b) Densitometric analysis of HEK293/27/UCOE clone. Increased expression of human rIFNγ messengers is observed in the 1B clone; in the case of HSP27 messengers, higher overexpression is observed in Clone 1A. Results are expressed as mean ± standard deviation of three samples. (c) Volumetric production of human rIFNγ during polyclonal and monoclonal selection. Results are expressed as mean ± standard error of two samples. (d) Human rIFNγ yields during polyclonal and monoclonal selection. Results are expressed as mean ± standard error of two samples. During polyclonal selection, a higher production of human rIFNγ was observed in Clone 2A, which was used for monoclonal selection, and the three clones with the highest production (1, 4, and 5) were chosen for further analysis.

the effect of the TOPO/HSP27 plasmid. The expression level in Pool 1A is 2.11 times higher than in the parental clone, with the HSP27 mRNA expression level at 1.27 ± 0.02 ARU. Meanwhile, the mRNA expression level of rIFNγ was highest in Pool 1B (1.12 ± 0.003 ARU).

Thus, Pool 3A was used for this purpose, with a titer of 15.25 ± 1.50 RU and a yield of 13.94 ± 1.37 RU/CV (see Figures 3(c) and 3(d)). Next, the six highest-yielding clones were selected (Figures 3(c) and 3(d)). When comparing the average titer and yield in both populations, a higher expression of the protein of interest was observed in the presence of both molecular markers (3.2- and 1.9-fold, respectively).

To further analyze the effect of these tools, three clones with the highest titer and yields were selected: Clone 1 (14.34 ± 2.83 RU and 7.00 ± 0.19 RU/VC), Clone 4 (21.18 ± 4.51 RU and 4.96 ± 0.050 RU/VC), and Clone 5 (11.98 ± 2.69 RU and 10.36 ± 0.02 RU/VC). These clones were designated as HEK/27/U-C1, HEK/27/U-C4, and HEK/27/U-C5.

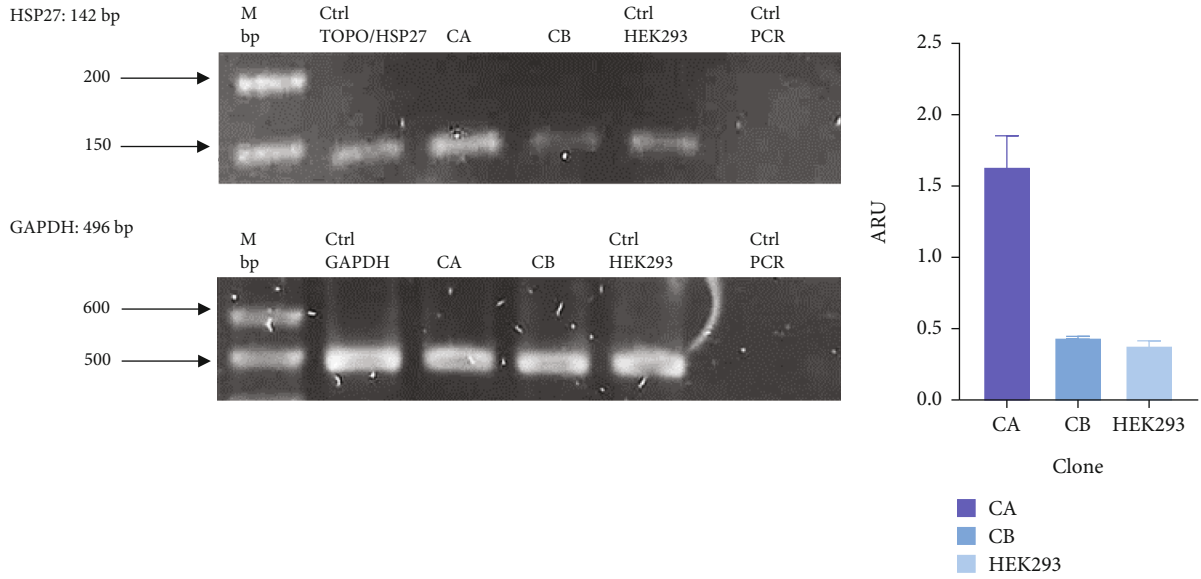

(a) Clone HEK293/HSP27

(b) HEK293/HSP27 densitometry

Figure 4: HEK293/HSP27 clonal evaluation. The presence of the gene human HSP27 of each clone was performed by RT-PCR. (a) HSP27 RT-PCR. CA: Clone A, CB: Clone B, Ctrl TOPO/HSP27: TOPO/HSP27 construct, Ctrl HEK293: nontransfected HEK293, Ctrl GAPDH: GAPDH constitutive gene. (b) Densitometric analysis of HEK293/HSP27 clone. Increased expression of HSP27 messengers was observed in the CA clone. Results are expressed as mean ± standard deviation of three samples.

3.2.3. HEK293/HSP27. Figure 4(a) shows the presence of HSP27 protein transcripts in the two clones derived from the monoclonal selection, with an amplicon of 142 bp observed in the CA and CB clones, as well as in the HEK293 Ctrl Lane (nontransfected cells). To verify overexpression due to the effect of TOPO/HSP27 vector transfection, densitometric analysis was performed (Figure 4(b)). The result shows that the level of HSP27 mRNA expression was higher in Clone CA (1.64 ± 0.22 ARU) compared to Clone CB (0.44 ± 0.009 ARU). The increase in HSP27 expression in Clones CA and CB was 4.1- and 1.1-fold higher, respectively, compared to the parental clone. Therefore, the CA clone was chosen for further analysis to generate the HEK293/HSP27/UCOE clone.

3.3. Effect of UCOE Elements and Overexpression of HSP27 Protein on the Growth and Biochemical Profile of the Clones Generated. Figure 5(a) shows the different growth patterns exhibited by the evaluated clones, and Table 2 summarizes the kinetic parameters. The growth rate (μ) was determined to be in the range of 0.0146–0.0233 h^{-1}, which is consistent with the values reported by [36] (0.014–0.023 h^{-1}) and [37] (0.020–0.029 h^{-1}) [36, 37] for this production platform. When comparing the three different clones, an increase in doubling time was observed relative to the parental line (HEK293).

In terms of maximum cell density achieved per batch, HEK/27 and HEK/27/U-C4 clones showed only a 1.2- and 1.1-fold increase over the parental HEK293 clone, which was not statistically significant (Table 2). Studies by Amini et al. overexpressed HSP27 in CHO cells to evaluate its effect on cell viability and growth. They observed a threefold increase in the peak viable cell density of clones transfected with HSP27 [38]. Therefore, the results obtained in the present study indicate a lower effect of HSP27 in human-derived cells compared to that reported with the murine platform. In fact, the HEK/27/U-C5 clone only reached a maximum density of 5.72×10^5 cell/mL in a small-scale culture.

On the other hand, the analysis of the metabolic profile was performed by determining the specific consumption and production rates of metabolites; lactate production rates from glucose were also calculated (Table 2). It can be observed that two of the rIFNγ-producing clones, HEK/27/U-C1 and HEK/27/U-C5, have the highest lactate production rates.

3.4. Effect of UCOE Elements and Overexpression of HSP27 Protein on the Production of Human rIFNγ. Regarding volumetric production, it was observed that the clones reached their highest concentration on the 12th day, including HEK/UCOE (control), HEK/27/U-C1, HEK/27/U-C4, and HEK/27/U-C5 (Figure 5(b)). Statistical analysis revealed that HEK/27/U-C5 clone exhibited a significant increase in volumetric production (51.25 ± 6.42 RU) compared to the rest of the clones. This clone also showed a similar effect in terms of Qp (Figure 5(c)), with a value of 96.05 ± 19.21 RU, which was 11.3 times higher with respect to the second most productive clone.

By correlating the metabolic profile and kinetic behavior, it can be concluded that the HEK/27/U-C5 clone demonstrates limited cell growth, focusing its metabolism on recombinant protein production rather than cell division.

3.4.1. Effect of UCOE Elements. When comparing the clone containing only the UCOE elements (HEK/UCOE) to those containing the HSP27 gene, the results show no

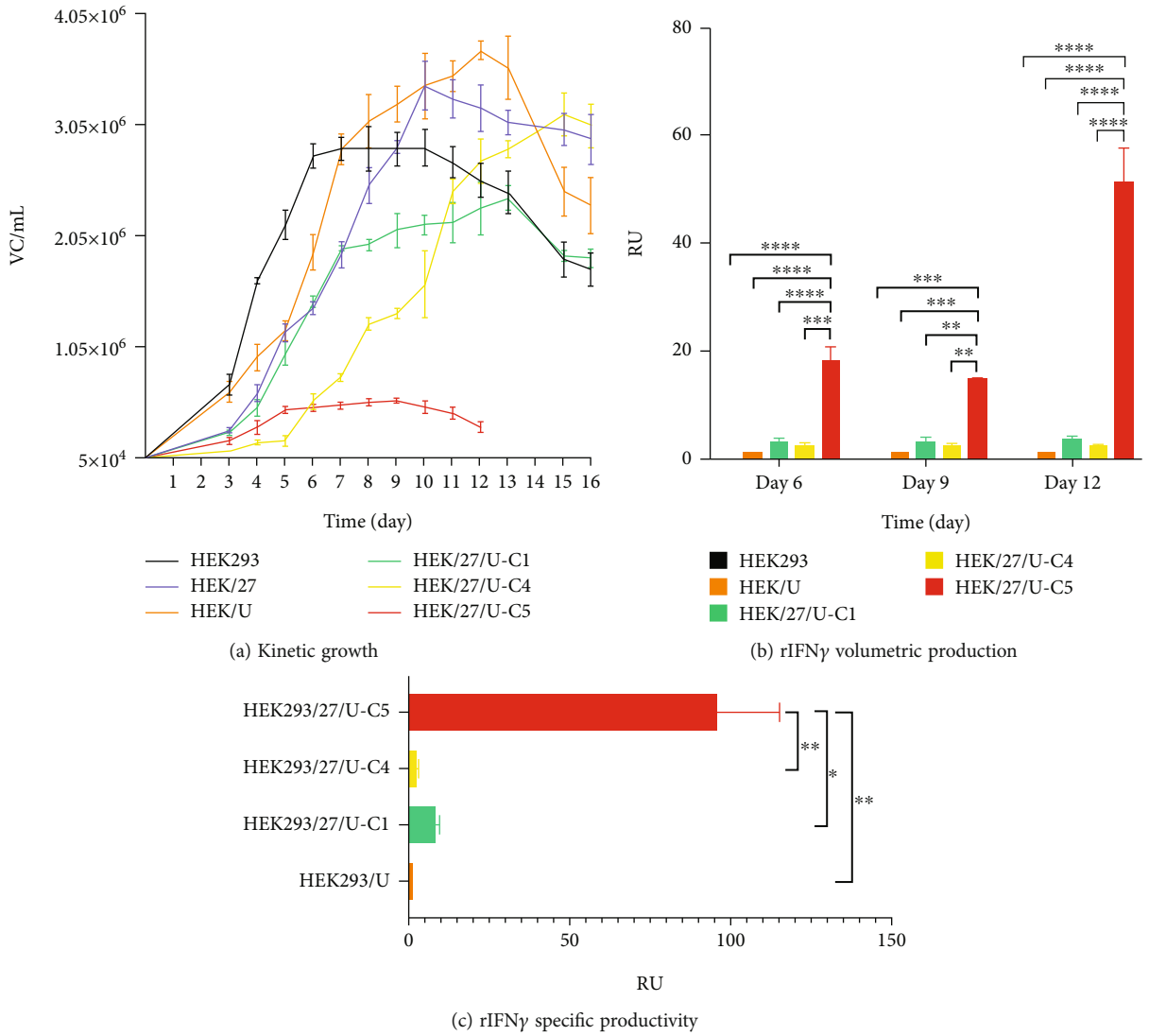

Figure 5: Growth kinetics of the HEK293 clones generated and volumetric production and specific productivity of human rIFNγ. (a) Growth kinetics were carried out in static cultures with DMEMF12 medium (10% FBS). Supernatant collection and cell counts were performed every 24 h. Results are expressed as mean ± standard deviation of six samples. (b) From the supernatants collected from Days 6, 9, and 12 of the growth kinetics/production kinetics of human rIFNγ, the volumetric production of the rIFNγ producing clones was evaluated. A two-way ANOVA ($p < 0.05$) and a Tukey analysis were performed as a post hoc test. (c) The specific productivity of human rIFNγ was evaluated from the supernatants collected from Days 6, 9, and 12 of the growth kinetics/production kinetics of human rIFNγ and the CV/mL presented at those times; the results show a significant difference between the production of clone HEK293/27/U-C5 and the rest of the clones. A one-way ANOVA ($p < 0.05$) and a Tukey analysis were performed as a post hoc test. The level of significance is taken at 0.05 or 5%. In both cases, results were expressed as the mean ± standard error of two samples. HEK293/HSP27 (HEK/27), HEK293/UCOE (HEK/U), HEK293/HSP27/UCOE-C1 (HEK/27/U-C1), HEK293/HSP27/UCOE-C4 (HEK/27/U-C4), HEK293/HSP27/UCOE-C5 (HEK/27/U-C5).

improvement in volumetric production or Qp of IFNγ (Figures 5(b) and 5(c)).

Several researchers have used CHO cells combined with UCOE elements for the stable production of recombinant proteins, achieving high expression levels [8, 39–41]. However, low levels of recombinant protein expression have also been reported in the CHO/UCOE cell combination compared to the use of other chromatin-modulating elements, such as STARs, MARs, and cHS4 [42].

In the case of HEK293 cells, there is limited evidence regarding the use of UCOE elements. However, Bandaranayake et al. reported an increase in the protein of interest [43], which contrast with the findings of [44], who observed lower expression levels compared to control cells or those produced by other chromatin-modulating elements [44]. The difference between the two experiments may lie in the molecular size of the UCOE elements used.

By compiling the data reported so far across various cell lines, the differences in the production levels of the model protein could be attributed to the size of the subfragment of the UCOE element used. Table 3 presents an analysis supporting this hypothesis. As observed, shorter fragments are

Table 2: Growth and biochemical profiles of producing HEK293 clones.

	HEK293	HEK/27	HEK/U	HEK/27/U-C1	HEK/27/U-C4	HEK/27/U-C5
Passage number	8	8	8	9	7	9
CD_{max} (CV/mL)	2.84×10^6	3.4×10^6	3.72×10^6	2.39×10^6	3.14×10^6	5.72×10^5
% viability	85	88	89	96	95	92
t_d (h)	29	44	36	34	40	38
μ (h^{-1})	0.0233	0.0157	0.020	0.0203	0.017	0.0182
qGlc (pmol/CV∗d)	−0.908 ± 0.303	−1.150 ± 0.046	−0.564 ± 0.110	−0.504 ± 0.060	−0.766 ± 0.013	−0.666 ± 0.062
qLac (pmol/CV∗d)	1.187 ± 0.339	2.392 ± 0.007	2.627 ± 0.018	2.612 ± 0.070	1.321 ± 0.051	3.692 ± 0.365
qGln (pmol/CV∗d)	−0.296 ± 0.002	−0.139 ± 0.008	−0.077 ± 0.005	−0.244 ± 0.030	−0.218 ± 0.006	−0.109 ± 0.002
qGlu (pmol/CV∗d)	−0.045 ± 0.001	−0.013 ± 0.002	−0.042 ± 0.008	−0.006 ± 0.001	−0.014 ± 0.001	0.140 ± 0.029
$Y_{Lac/Glc}$ (qLac/qGlc)	1.33 ± 0.069	2.08 ± 0.089	4.853 ± 0.979	5.269 ± 0.768	1.72 ± 0.037	5.539 ± 0.030

Note: Maximum cell density: CD_{max}; % of viability: percentage of viability reached at the end of the kinetics; time of duplication: t_d; specific growth rate: μ; q: specific consumption rate; pmol/CV∗D: picomole/viable cell∗day. Signs (−) indicate metabolite consumption. Signs (+) indicate metabolite production. Abbreviations: Glc, glucose; Gln, glutamine; Glu, glutamate; Lac, lactate.

Table 3: Analysis of different fragments and size of UCOE elements.

UCOE subfragment	Cell line	Model protein	Level of production	Reference
8 Kb	CHO-K1	IgG	↓	[45]
4 Kb	CHO-S	TRAIL R2	↑	[46]
4 Kb	CHO-S	h-TG2	↑	[46]
4 Kb	Mouse embryonic stem cells	GFP	↓	[47]
4 Kb	HEK293	hIFNγ	↓	"Present work"
3.2 Kb	CHO-K1	IgG	↑	[45]
3.2 Kb	CHO-K1	IgG	↑	[45]
3.2 Kb	BHK21	Factor VIII	↓	[48]
1.5 Kb	CHO-DG44	TNFα	↑	[8]
1.5 Kb	BHK21	Factor VIII	↑	[48]
1.5 Kb	Mouse embryonic stem cells	GFP	↑	[47]
0.7 Kb	Mouse embryonic stem cells	GFP	↑↑	[47]
0.7 Kb	HEK293F	GFP	↑	[43]

Note: Production levels were determined with respect to the control clone used in each article.
Abbreviations: GFP, green fluorescent protein; hIFNγ, human interferon gamma; h-TG2, human transglutaminase 2; IgG, immunoglobulin G; TNFα, tumor necrosis factor α; TRAIL R2, human tumor necrosis factor-related apoptosis-inducing ligand R2.

more effective in preventing silencing and confer higher expression of the protein of interest, provided that this region belongs to the CBX3 locus [47]. However, this is not a universal rule, and further data are needed to confirm this conclusion.

Therefore, in the present work, using a 4-Kb UCOE element, with a portion of the promoters divergently transcribed from HNRPA2B1 and CBX3, helps explain the absence of a positive effect on the increase in production. This result complements the data in Table 3 for the HEK293 platform. Further studies using fragments smaller than 1.5 Kb are recommended to confirm this trend across other production systems.

3.4.2. Effect of HSP27 Protein Overexpression. The results show that clones overexpressing human HSP27 exhibit higher IFNγ production. The average of the six clones with the PCD-modulating protein shows a 3.22-fold higher titer compared to the average of the clones containing only the UCOE elements. In terms of yield, this increase is 1.92-fold. When analyzing the specific productivity of the highest-yielding clones from each population (HEK/U vs. HEK/27/U-C5), it was found to be 96-fold higher.

This behavior could be attributed to the antiapoptotic and chaperone characteristics of HSP27, which is consistent with the findings reported by [21, 22]. Their results demonstrate that overexpression of murine HSP27 in CHO cells enhances apoptosis resistance and increases cell production. Both studies reported enhanced model protein expression as well as delayed activity of caspases 2, 3, 8, and 9 [21, 22].

When analyzing the growth kinetics of the clones overexpressing HSP27 (Figure 5(a)), it was observed that a relatively constant viable cell density was maintained during the stationary phase, compared to the parental cells and the HEK/U clone, which showed a constant decline in viable cell density starting from Day 10 to 12, respectively. This effect

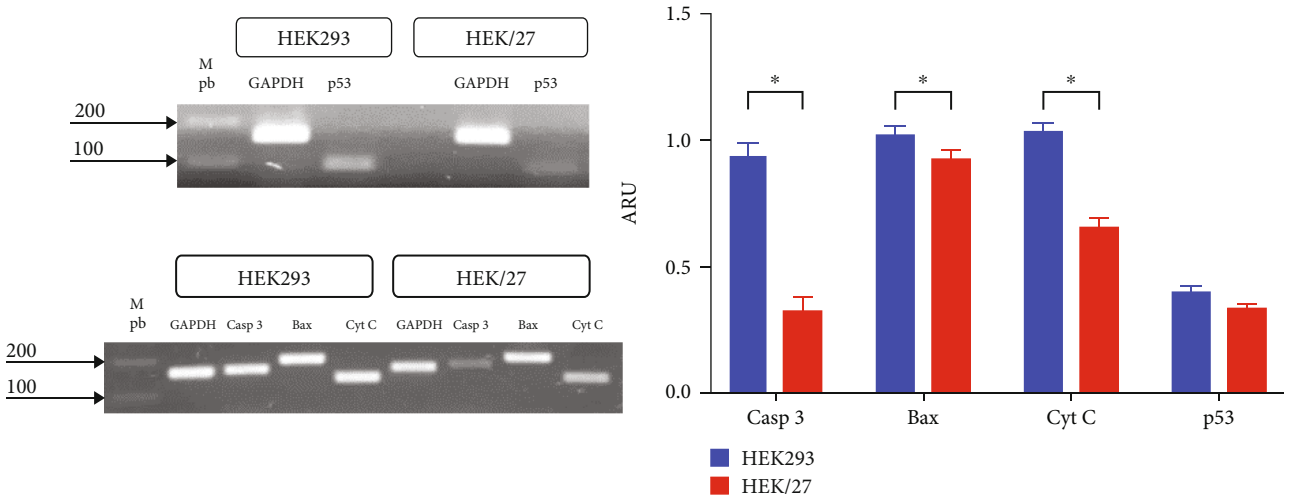

(a) Apoptosis genes and p53 RT-PCR

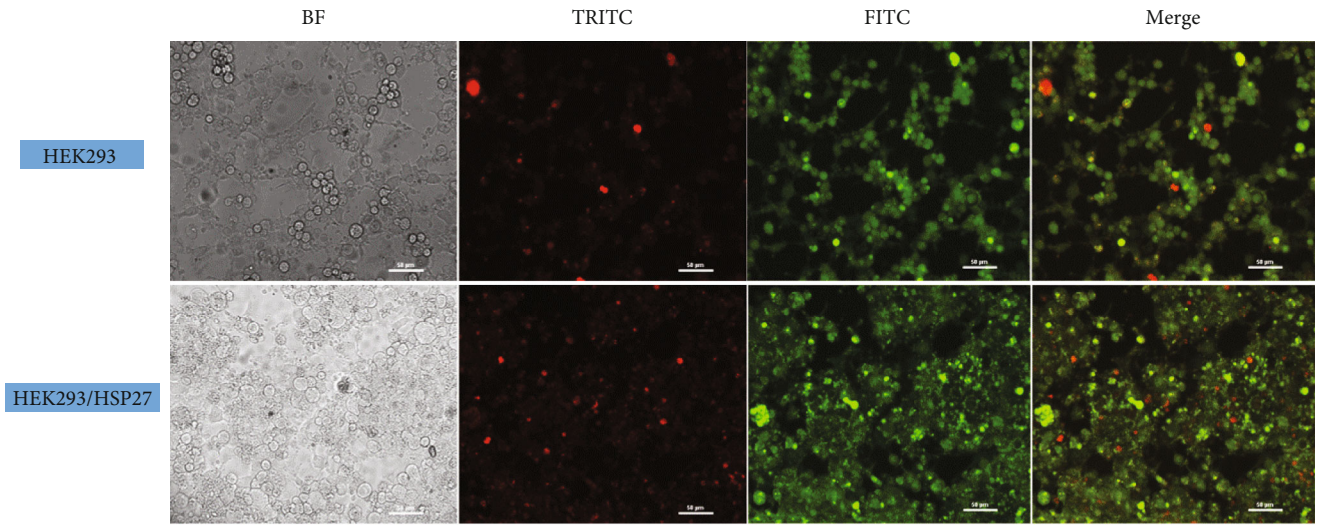

(b) Apoptosis analysis by acridine orange/propidium iodide staining

FIGURE 6: Apoptosis detection. (a) RT-PCR of caspase 3, Bax, cytochrome C, and p53 genes shows significant differences in the expression of these genes between HEK and HEK293/HSP27 (HEK/27) cells, except for p53. Results represent mean ± standard deviation of three samples, and a Mann–Whitney analysis was performed ($p < 0.05$). The level of significance is taken at 0.05 or 5%. (b) Apoptosis analysis was performed by staining cells with acridine orange/propidium iodide. Cells were observed under a Nikon eclipse E400 epifluorescence microscope with 20 × objective.

could positively impact the batch culture lifetime, potentially increasing the volumetric production of the protein of interest.

It is worth mentioning that, in all cases, approximately 85% viability was obtained at the end of culture (Table 2). However, this was relative to the viable cell density at the end of the culture. This effect may be attributed to the autophagic characteristic of HEK293 cells [49]. To further analyze the activity of HSP27 on PCD, the following studies were performed.

3.5. Overexpression of HSP27 Protein Exerts an Effect on the Modulation of Apoptosis and Autophagy

3.5.1. Apoptosis Assays. A possible modulation of apoptosis was analyzed at the transcriptional level by RT-PCR, monitoring the gene expression of caspase 3, Bax, cytochrome C, and p53 (Figure 6(a)). The result demonstrated a significant downregulation of messenger RNA expression in the HEK/27 clone compared to the parental HEK293 clone, except for p53.

DNA damage activates p53 and its downstream target genes, which can lead to either apoptosis or cell survival, through mechanisms such as cell cycle arrest or DNA repair. The roles of HSP27 in p53-mediated cellular responses to DNA damage remain controversial [50]. Some studies suggest that HSP27, depending on its phosphorylation status, plays different roles in regulating the p53 pathway and cell survival. Others research indicates that negative regulation of HSP27 is associated with activation of the p53 pathway [50–52].

Numerous studies support the obtained data, as it is known that HSP27 positively regulates the PI3-activating kinase Akt, which interacts with Bax (Akt/Bax). This

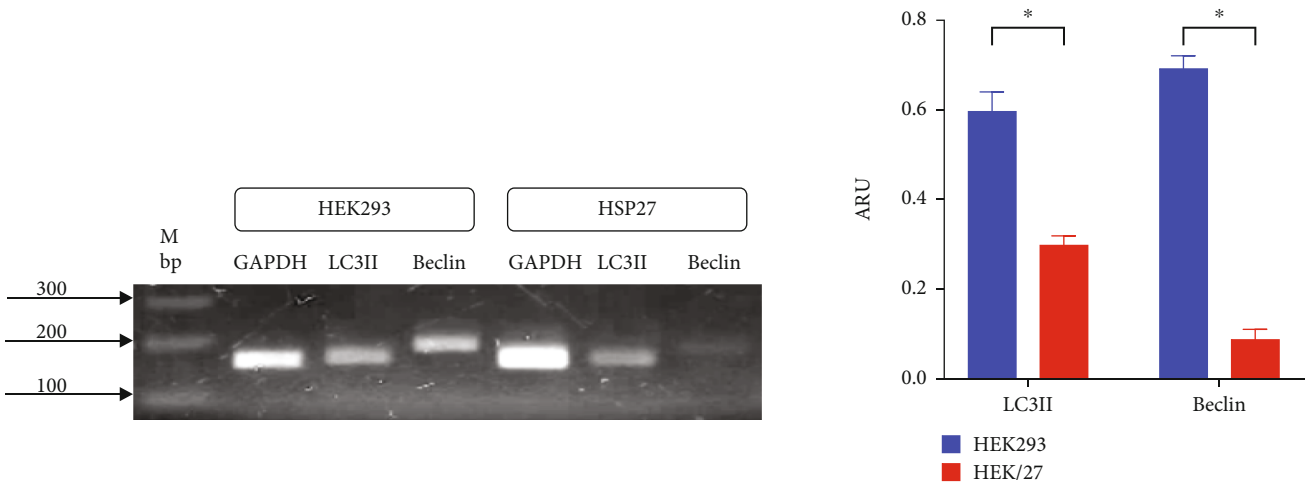

(a) RT-PCR of LC3II and Beclin 1

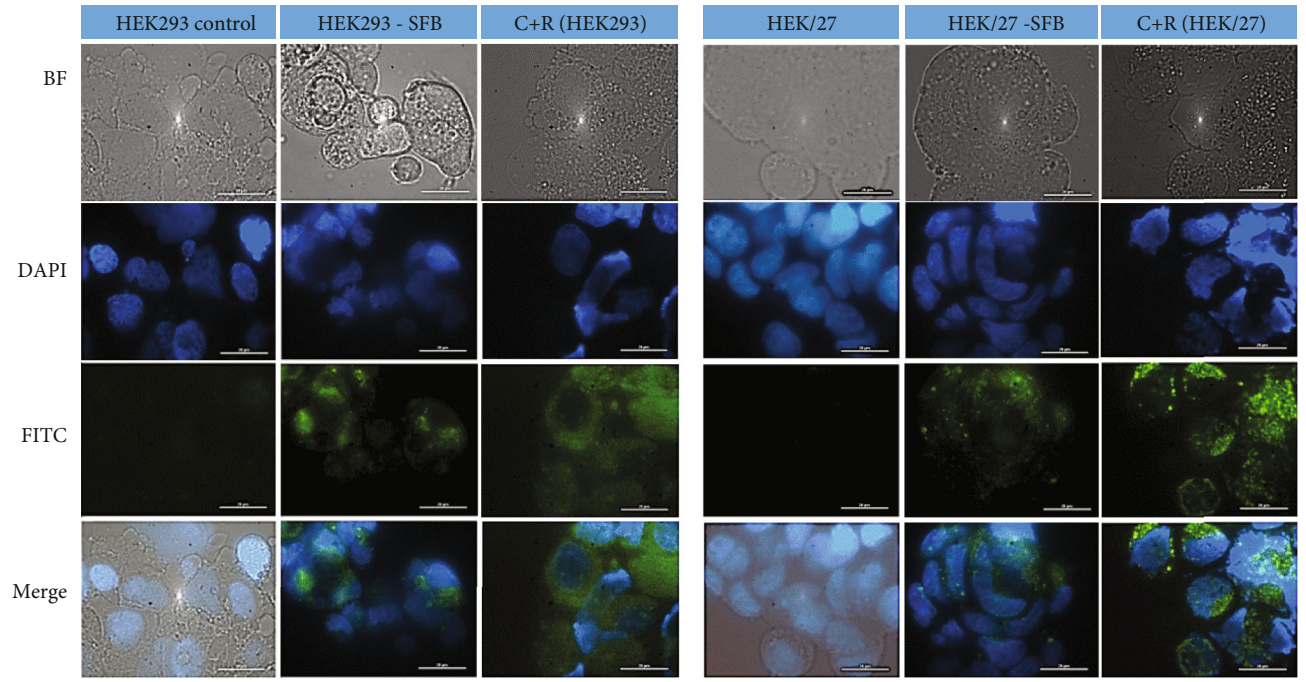

(b) Autophagy analysis by autophagosome detection

Figure 7: Autophagy detection. (a) RT-PCR of LC3II and Beclin 1 genes shows significant differences in the expression between HEK293 and HEK293/HSP27 (HEK/27) cells. Results represent mean ± standard deviation of three samples, and a Mann–Whitney analysis was performed ($p < 0.05$). The level of significance is taken at 0.05 or 5%. (b) Autophagy analysis was performed by autophagosome detection using the Autophagy Detection Kit (Abcam, ab139484). Nuclei are shown in blue (Hoechst dye, DAPI filter) and autophagic vacuoles (autophagosomes) are shown in green (FITC filter). Cells were observed under a Nikon eclipse E400 epifluorescence microscope with 100× objective.

interaction blocks the translocation of Bax to mitochondria, preventing the release of cytochrome C [53]. Additionally, HSP27 interacts with cytochrome C and caspase 3, inactivating them [54]. These molecular mechanisms enable HSP27 to modulate apoptosis, which explains the observed decrease in its expression. Furthermore, it has been reported that this function promotes greater cell survival, correlating with the findings in its kinetic profile. However, the same effect was expected for p53, as HSP27 is known to inactivate this gene [55]. Although the results show a decrease in p53 expression, these changes are not statistically significant.

The effect was also monitored by epifluorescence microscopy. Figure 6(b) shows the results of AO and PI staining of HEK293 and HEK/27 cells treated with STS. STS is known to be one of the most potent and widely used proapoptotic stimuli, as it causes inactivation of factors such as eIF4F and eIF2α, as well as protein kinases like p70S6, which are critical for mRNA translation control [56]. STS can induce apoptosis through both the mitochondrial and endoplasmic reticulum stress pathway. Studies have shown that cells with overexpressing apoptosis inhibitors, such as Bcl-2 and Bcl-x(L), when treated

with STS, only attenuate but do not completely prevent STS-induced apoptosis [57].

As shown, red nuclei were observed, indicating compromised cell membrane integrity. Morphological features consistent with a PCD process were also identified, including DNA condensation, the presence of intracellular vacuolization, loss of adhesion, nuclear fragmentation, and loss of cytoplasmic structure [58].

3.5.2. Autophagy Detection. To determine whether HSP27 overexpression affects autophagic flux, RT-PCR analysis of Beclin 1 and LC3II was performed, along with fluorescence microscopy in HEK293 and HEK/27 cells. In the autophagy process, proteins such as Beclin 1 and LC3II play a key role, as they are essential for the autophagosome formation. For this reason, they are widely accepted as key markers of autophagic activity [59].

RT-PCR analysis for Beclin 1 and LC3II (Figure 7(a)) reveals that mRNA expression of both genes is significantly lower in clone HEK/27 compared to clone HEK293. Although Beclin 1 levels are reduced, it is notable that LC3II levels do not decrease drastically. This observation aligns with studies conducted by Quiles et al. [60], which indicated that autophagosome formation in response to stress can occur independently of Beclin 1 [60].

Figure 7(b) shows the fluorescence microphotographs, where nuclei appear in blue (Hoechst dye, DAPI filter), and autophagic vacuoles (autophagosomes) are shown in green (FITC filter). Rapamycin was used a positive control due to its strong autophagy-inducing properties, while chloroquine served as an inhibitor of autophagosomes degradation to allow their visualization [61, 62]. As expected, in the positive controls for both cell line, autophagosomes are distributed throughout the perinuclear region and cytoplasm. However, upon exposing HEK293 and HEK/27 cells to a mild inducer (FBS deprivation), autophagosomes were predominantly concentrated in the perinuclear region. When comparing the fluorescence intensity and therefore the abundance of autophagosomes, it was notably lower in HEK/27 cells. This observation suggests that HSP27 may protect the cells from undergoing autophagy under the experimental conditions analyzed.

These results suggest that HSP27 downregulates both Beclin 1 and LC3II and exhibits an apparent decrease in autophagosome formation when exposed to a nutrient-deficient environment, such as FBS deprivation. Although this type of PCD is uncommon during bioprocessing, HEK293 cells have the capacity to activate this pathway in the final stage of a batch culture. Therefore, HSP27 appears to exert a modulatory effect on autophagy, leading to metabolic change that enhances the production of recombinant protein.

4. Conclusion

In the present study, the effects of UCOE elements and overexpression of human HSP27 protein on the production of human IFNγ produced in batch cultures of HEK293 cells were evaluated. The results demonstrated that the generated clones (HEK293/HSP27, HEK293/UCOE, and HEK293/HSP27/UCOE) exhibit different growth patterns compared to the parental HEK293 clone.

The HEK293/UCOE clone showed the lowest volumetric production, suggesting that the size of UCOE element (4 Kb) plays a critical role and may not be ideal for the HEK293 system in this context. In contrast, clones overexpressing HSP27 protein exhibit significantly higher volumetric production (51.24 ± 9.08 UR at 12 days) and Qp (96.05 ± 27.17 UR) indicating a direct relationship between the overexpression of this PCD modulator protein and increased recombinant protein production. These findings correlate with a decrease in Bax, caspase 3, and cytochrome C transcripts in the apoptosis study, as well as a reduction in Beclin 1 and LC3II levels in the autophagy analysis. This study highlights the utility of a molecular strategy based on the overexpression of human HSP27 protein to develop HEK293 cell lines with enhanced recombinant protein production capabilities.

Data Availability Statement

Data will be made available upon request to the corresponding author.

Disclosure

A preprint has previously been previously published in Authorea [63]; the link to access is as follows: doi:10.22541/au.172114891.12105911/v1.

Conflicts of Interest

The authors declare no conflicts of interest.

Funding

Thanks are due to CONACyT (CB-2015/257408) for their financial support and to CONACyT-INFR-2014 for their support through project 226271 and for the postgraduate grant awarded (665604).

Acknowledgments

The authors acknowledge CONAHCyT for the financial support by the following projects: CB-2015/257408 and CONAHCyT-INFR-2014/226271. Concepción Sosa–García thanks CONAHCyT for the PhD grant 665604.

Supporting Information

Additional supporting information can be found online in the Supporting Information section. *(Supporting Information)* The supporting information contains the sequencing alignments of the UCOE/IFNγ and TOPO/HSP27 vectors. These were performed using the BLAST program from NCBI. Figure S1. The alignment of IFNγ contained in the UCOE/IFNγ vector with the data recorded in the NCBI database is shown. It is observed that there is 100% identity with the coding region of the human IFNγ. Figure S2. The alignment of HSP27 (HSPB1) contained in the TOPO/HSP27

vector with the data recorded in the NCBI database is shown. It is observed that there is 100% identity with the coding region of human HSP27.

References

[1] G. Walsh and E. Walsh, "Biopharmaceutical benchmarks 2022," *Nature Biotechnology*, vol. 40, no. 12, pp. 1722–1760, 2022.

[2] N. I. Majewska, M. L. Tejada, M. J. Betenbaugh, and N. Agarwal, "N-Glycosylation of IgG and IgG-like recombinant therapeutic proteins: why is it important and how can we control it?," *Annual Review of Chemical and Biomolecular Engineering*, vol. 11, no. 1, pp. 311–338, 2020.

[3] J. K. K. Mark, C. S. Y. Lim, F. Nordin, and G. J. Tye, "Expression of mammalian proteins for diagnostics and therapeutics: a review," *Molecular Biology Reports*, vol. 49, no. 11, pp. 10593–10608, 2022.

[4] B. Handyside, A. M. Ismail, L. Zhang et al., "Vector genome loss and epigenetic modifications mediate decline in transgene expression of AAV5 vectors produced in mammalian and insect cells," *Molecular Therapy*, vol. 30, no. 12, pp. 3570–3586, 2022.

[5] J. Zimak, Z. W. Wagoner, N. Nelson et al., "Epigenetic silencing directs expression heterogeneity of stably integrated multitranscript unit genetic circuits," *Scientific Reports*, vol. 11, no. 1, p. 2424, 2021.

[6] R. E. Sizer and R. J. White, "Use of ubiquitous chromatin opening elements (UCOE) as tools to maintain transgene expression in biotechnology," *Computational and Structural Biotechnology Journal*, vol. 21, pp. 275–283, 2023.

[7] J. J. Neville, J. Orlando, K. Mann, B. McCloskey, and M. N. Antoniou, "Ubiquitous chromatin-opening elements (UCOEs): applications in biomanufacturing and gene therapy," *Biotechnology Advances*, vol. 35, no. 5, pp. 557–564, 2017.

[8] C. C. Doan, T. L. Le, N. Q. C. Ho, and N. S. Hoang, "Effects of ubiquitous chromatin opening element (UCOE) on recombinant anti-TNFα antibody production and expression stability in CHO-DG44 cells," *Cytotechnology*, vol. 74, no. 1, pp. 31–49, 2022.

[9] R. Hoseinpoor, B. Kazemi, M. Rajabibazl, and A. Rahimpour, "Improving the expression of anti-IL-2Rα monoclonal antibody in the CHO cells through optimization of the expression vector and translation efficiency," *Journal of Biotechnology*, vol. 324, no. 75, pp. 112–120, 2020.

[10] K. A. Skipper, A. K. Hollensen, M. N. Antoniou, and J. G. Mikkelsen, "Sustained transgene expression from sleeping beauty DNA transposons containing a core fragment of the HNRPA2B1-CBX3 ubiquitous chromatin opening element (UCOE)," *BMC Biotechnology*, vol. 19, no. 1, p. 75, 2019.

[11] Z. Li, Z. Fan, X. Wang, and T. Wang, "Factors affecting the expression of recombinant protein and improvement strategies in Chinese hamster ovary cells," *Frontiers in Bioengineering and Biotechnology*, vol. 10, pp. 1–12, 2022.

[12] T. A. Arena, B. Chou, P. D. Harms, and A. W. Wong, "An anti-apoptotic HEK293 cell line provides a robust and high titer platform for transient protein expression in bioreactors," *MAbs*, vol. 11, no. 5, pp. 977–986, 2019.

[13] F. Safari and B. Akbari, "Knockout of caspase-7 gene improves the expression of recombinant protein in CHO cell line through the cell cycle arrest in G2/M phase," *Biological Research*, vol. 55, no. 1, pp. 2–8, 2022.

[14] K. Xiong, K. Marquart, K. La Cour et al., "Reduced apoptosis in Chinese hamster ovary cells via optimized CRISPR interference," *Biotechnology and Bioengineering*, vol. 116, no. 7, pp. 1813–1819, 2019.

[15] S. Gülce, B. Calimlioglu, and S. Deliloglu, "Using Bcl-xL anti-apoptotic protein for altering target cell apoptosis," *Electronic Journal of Biotechnology*, vol. 15, no. 5, pp. 1–8, 2012.

[16] S. Lee and G. M. Lee, "Bcl-2 overexpression in CHO cells improves polyethylenimine-mediated gene transfection," *Process Biochemistry*, vol. 48, no. 9, pp. 1436–1440, 2013.

[17] J. M. Pemberton, D. Nguyen, E. J. Osterlund et al., "The carboxyl-terminal sequence of PUMA binds to both anti-apoptotic proteins and membranes," *Elife*, vol. 12, 2023.

[18] A. A. Patil, S. A. Bhor, and W. J. Rhee, "Cell death in culture: molecular mechanisms, detections, and inhibition strategies," *Journal of Industrial and Engineering Chemistry*, vol. 91, pp. 37–53, 2020.

[19] E. R. Gallagher and E. L. Holzbaur, "The selective autophagy adaptor p62/SQSTM1 forms phase condensates regulated by HSP27 that facilitate the clearance of damaged lysosomes via lysophagy," *Cell Reports*, vol. 42, no. 2, Article ID 112037, 2023.

[20] B. Penke, F. Bog, and T. Crul, "Heat shock proteins and autophagy pathways in neuroprotection: from molecular bases to pharmacological interventions," *International Journal of Molecular Sciences*, vol. 19, no. 1, p. 325, 2018.

[21] Y. Lee, K. Wong, J. Tan et al., "Overexpression of heat shock proteins (HSPs) in CHO cells for extended culture viability and improved recombinant protein production," *Journal of Biotechnology*, vol. 143, no. 1, pp. 34–43, 2009.

[22] J. Tan, Y. Lee, T. Wang, M. Yap, T. Tan, and S. Ng, "Heat shock protein 27 overexpression in CHO cells modulates apoptosis pathways and delays activation of caspases to improve recombinant monoclonal antibody titre in fed-batch bioreactors," *Biotechnology Journal*, vol. 10, no. 5, pp. 790–800, 2015.

[23] M. Pulix, V. Lukashchuk, D. C. Smith, and A. J. Dickson, "Molecular characterization of HEK293 cells as emerging versatile cell factories," *Current Opinion in Biotechnology*, vol. 71, pp. 18–24, 2021.

[24] C. A. Tavira-Montalvan, A. Garcia-Gonzalez, and A. Meneses-Acosta, "Characterization and analysis of HEK293/adenovirus type 5 cell cultures under simulated microgravity using differential neural network modeling," *BioMed Research International*, vol. 2023, no. 1, Article ID 8836756, 2023.

[25] F. Graham and J. Smiley, "Characteristics of a human cell line transformed by DNA from human adenovirus type 5," *The Journal of General Virology*, vol. 36, no. 1, pp. 59–72, 1977.

[26] P. A. Olsen and S. Krauss, "The adenoviral E1B-55k protein present in HEK293 cells mediates abnormal accumulation of key WNT signaling proteins in large cytoplasmic aggregates," *Genes*, vol. 12, no. 12, p. 1920, 2021.

[27] J. Hu, J. Han, H. Li et al., "Human embryonic kidney 293 cells: a vehicle for Biopharmaceutical Manufacturing, Structural Biology, and Electrophysiology: state of the art and future perspectives," *Cells Tissues Organs*, vol. 205, no. 1, pp. 1–8, 2018.

[28] M. Malm, R. Saghaleyni, M. Lundqvist et al., "Evolution from adherent to suspension: systems biology of HEK293 cell line development," *Scientific Reports*, vol. 10, no. 1, pp. 1–15, 2020.

[29] R. R. Zhang, N. N. Meng, C. Liu et al., "PDB-1 from Potentilla discolor Bunge induces apoptosis and autophagy by downregulating the PI3K/Akt/mTOR signaling pathway in A549 cells," *Biomedicine and Pharmacotherapy*, vol. 129, Article ID 110378, 2020.

[30] A. I. Giotakis, C. K. Kontos, L. D. Manolopoulos, A. Sismanis, M. M. Konstadoulakis, and A. Scorilas, "High BAX/BCL2 mRNA ratio predicts favorable prognosis in laryngeal squamous cell carcinoma, particularly in patients with negative lymph nodes at the time of diagnosis," *Clinical Biochemistry*, vol. 49, no. 12, pp. 890–896, 2016.

[31] Y. Kang, Y. Sun, Y. Zhang, and Z. Wang, "Cytochrome c is important in apoptosis of labial glands in primary Sjogren's syndrome," *Molecular Medicine Reports*, vol. 17, no. 1, pp. 1993–1997, 2018.

[32] D. Gao, X. Yu, B. Zhang et al., "Role of autophagy in inhibiting the proliferation of A549 cells by type III interferon," *Cell Biology International*, vol. 43, no. 6, pp. 605–612, 2019.

[33] H. Guo, H. Ding, X. Tang et al., "Quercetin induces pro-apoptotic autophagy via SIRT1/AMPK signaling pathway in human lung cancer cell lines A549 and H1299 in vitro," *Thoracic Cancer*, vol. 12, no. 9, pp. 1415–1422, 2021.

[34] X. S. Zhang, K. Y. Wang, J. Q. Gao, R. J. Li, Q. B. Guan, and L. Song, "Study on the expression of p53 and MMP-2 in patients with lung cancer after interventional therapy," *Oncology Letters*, vol. 16, no. 4, pp. 4291–4296, 2018.

[35] N. Kwon, K. E. Lee, M. Singh, and S. G. Kang, "Suitable primers for GAPDH reference gene amplification in quantitative RT-PCR analysis of human gene expression," *Gene Reports*, vol. 24, Article ID 101272, 2021.

[36] M. Jang, E. S. Pete, and P. Bruheim, "The impact of serum-free culture on HEK293 cells: from the establishment of suspension and adherent serum-free adaptation cultures to the investigation of growth and metabolic profiles," *Frontiers in Bioengineering and Biotechnology*, vol. 10, pp. 1–16, 2022.

[37] S. Seidel, R. W. Maschke, F. Mozaffari, R. Eibl-Schindler, and D. Eibl, "Improvement of HEK293 cell growth by adapting hydrodynamic stress and predicting cell aggregate size distribution," *Bioengineering*, vol. 10, no. 4, p. 478, 2023.

[38] M. R. Amini, A. Rahimpour, R. Hoseinpoor, and M. Rajabibazl, "Expression of the mouse HSP27 chaperone in CHO-K1 cells for the enhancement of viable cell density in batch culture," *Trends in Peptide and Protein Sciences*, vol. 7, no. e2, pp. 10–14, 2022.

[39] Z. Betts and A. J. Dickson, "Assessment of UCOE on recombinant EPO production and expression stability in amplified Chinese hamster ovary cells," *Molecular Biotechnology*, vol. 57, no. 9, pp. 846–858, 2015.

[40] F. Nematpour, F. Mahboudi, B. Vaziri et al., "Evaluating the expression profile and stability of different UCOE containing vector combinations in mAb-producing CHO cells," *BMC Biotechnology*, vol. 17, no. 1, pp. 17-18, 2017.

[41] F. Saunders, B. Sweeney, M. N. Antoniou, P. Stephens, and K. Cain, "Chromatin function modifying elements in an industrial antibody production platform-comparison of UCOE, MAR, STAR and cHS4 elements," *PLoS One*, vol. 10, no. 4, pp. 1–20, 2015.

[42] A. P. Otte, T. H. J. Kwaks, R. J. M. BloklandVan et al., "Various expression-augmenting DNA elements benefit from STAR-Select, a novel high stringency selection system for protein expression," *Biotechnology Progress*, vol. 23, no. 4, pp. 801–807, 2007.

[43] A. D. Bandaranayake, C. Correnti, B. Y. Ryu, M. Brault, R. K. Strong, and D. J. Rawlings, "Daedalus: a robust, turnkey platform for rapid production of decigram quantities of active recombinant proteins in human cell lines using novel lentiviral vectors," *Nucleic Acids Research*, vol. 39, no. 21, p. e143, 2011.

[44] Y. Mao, R. Yan, A. Li et al., "Lentiviral vectors mediate long-term and high efficiency transgene expression in HEK 293T cells," *International Journal of Medical Sciences*, vol. 12, no. 5, pp. 407–415, 2015.

[45] J. J. C. Hou, B. S. Hughes, M. Smede et al., "High-throughput ClonePix FL analysis of mAb-expressing clones using the UCOE expression system," *New Biotechnology*, vol. 31, no. 3, pp. 214–220, 2014.

[46] S. Boscolo, F. Mion, M. Licciulli et al., "Simple scale-up of recombinant antibody production using an UCOE containing vector," *New Biotechnology*, vol. 29, no. 4, pp. 477–484, 2012.

[47] N. Gödecke, S. Herrmann, V. Weichelt, and D. Wirth, "A ubiquitous chromatin opening element and DNA demethylation facilitate doxycycline-controlled expression during differentiation and in transgenic mice," *ACS Synthetic Biology*, vol. 12, no. 2, pp. 482–491, 2023.

[48] A. R. Nair, X. Jinger, and T. W. Hermiston, "Effect of different UCOE-promoter combinations in creation of engineered cell lines for the production of Factor VIII," *BMC Research Notes*, vol. 4, no. 1, p. 178, 2011.

[49] P. Musiwaro, M. Smith, M. Manifava, S. A. Walker, and N. T. Ktistakis, "Characteristics and requirements of basal autophagy in HEK 293 cells," *Autophagy*, vol. 9, no. 9, pp. 1407–1417, 2013.

[50] Y. Xu, Y. Diao, S. Qi et al., "Phosphorylated Hsp27 activates ATM-dependent p53 signaling and mediates the resistance of MCF-7 cells to doxorubicin-induced apoptosis," *Cellular Signalling*, vol. 25, no. 5, pp. 1176–1185, 2013.

[51] E. V. Kaigorodova, L. S. Litvinova, E. V. Konovalova et al., "The inhibition of Hsp27 chaperone affects the level of p53 protein in tumor cells," *International Journal of Biology*, vol. 5, no. 3, pp. 13–18, 2013.

[52] C. O'Callaghan-Sunol, V. L. Gabai, and M. Y. Sherman, "Hsp27 modulates p53 signaling and suppresses cellular senescence," *Cancer Research*, vol. 67, no. 24, pp. 11779–11788, 2007.

[53] A. Havasi, Z. Li, Z. Wang et al., "Hsp27 inhibits Bax activation and apoptosis via a phosphatidylinositol 3-kinase-dependent mechanism," *The Journal of Biological Chemistry*, vol. 283, no. 18, pp. 12305–12313, 2008.

[54] C. Concannon, S. Orrenius, and A. Samali, "Hsp27 inhibits cytochrome c -mediated caspase activation by sequestering both pro-caspase-3 and cytochrome c," *Gene Expression*, vol. 9, no. 4, pp. 195–201, 2001.

[55] M. Lampros, N. Vlachos, S. Voulgaris, and G. A. Alexiou, "The role of Hsp27 in chemotherapy resistance," *Biomedicines*, vol. 10, no. 4, p. 897, 2022.

[56] A. R. Tee and C. G. Proud, "Staurosporine inhibits phosphorylation of translational regulators linked to mTOR," *Cell Death and Differentiation*, vol. 8, no. 8, pp. 841–849, 2001.

[57] J. Manns, M. Daubrawa, S. Driessen et al., "Triggering of a novel intrinsic apoptosis pathway by the kinase inhibitor staurosporine: activation of caspase-9 in the absence of Apaf-1," *The FASEB Journal*, vol. 25, no. 9, pp. 3250–3261, 2011.

[58] L. Galluzzi, I. Vitale, S. A. Aaronson et al., "Molecular mechanisms of cell death: recommendations of the Nomenclature

Committee on Cell Death 2018," *Cell Death and Differentiation*, vol. 25, no. 3, pp. 486–541, 2018.

[59] N. Nurdinov, V. Çınar, A. Güler, S. Yılmaz, N. Delibaşı Kökçü, and Z. Hamurcu, "LC3 and Beclin-1 as markers of autophagic activity in breast cancer," *Journal of Clinical Practice and Research*, vol. 43, no. 4, pp. 333–336, 2020.

[60] J. M. Quiles, R. H. Najor, E. Gonzalez et al., "Deciphering functional roles and interplay between Beclin1 and Beclin2 in autophagosome formation and mitophagy," *Science Signaling*, vol. 16, no. 770, Article ID eabo4457, 2023.

[61] X. Lin, L. Han, J. Weng, K. Wang, and T. Chen, "Rapamycin inhibits proliferation and induces autophagy in human neuroblastoma cells," *Bioscience Reports*, vol. 38, no. 6, pp. 1–8, 2018.

[62] O. Tusskorn, T. Khunluck, A. Prawan, L. Senggunprai, and V. Kukongviriyapan, "Mitochondrial division inhibitor-1 potentiates cisplatin-induced apoptosis via the mitochondrial death pathway in cholangiocarcinoma cells," *Biomedicine & Pharmacotherapy*, vol. 111, pp. 109–118, 2019.

[63] C. Sosa-García, U. A. Sánchez-Pacheco, C. A. Tavira-Montalván, and A. Meneses-Acosta, *Expression of UCOE and HSP27 Molecular Elements to Improve the Stable Protein Production on HEK293 Cells*, Authorea, 2024.